Chapter 7

Adsorption using mould

7.1 Removal of Cu^{2+}, Ni^{2+} and Zn^{2+} ions by Mould

The occurrence of heavy metals in soil is strongly influenced by the region's environmental conditions and rock types. Thermal power plants, battery industry, smelting operations, mining and electroplating introduce heavy metals like copper, nickel and zinc into the water supply [2], [469]. Beyond a certain concentration, heavy metals can be toxic. Nickel, copper and zinc have an oral limit of 0.25 mg/ day, 2.5 mg/ day [470] and zinc 11 mg/day respectively [40]. Diarrhoea, difficulty in breathing, fever, urinary retention, metallic taste, seizures, vomiting and jaundice are caused by zinc poisoning [469], [471]. Copper is beneficial to humans, but excessive amounts results in headaches, fever, hematemesis, diarrhoea, abdominal cramps, Kayser-Fleischer rings and jaundice. It is particularly harmful to people who have Wilson's disease [470]. Long-term exposure of nickel has been linked to contact dermatitis, lung cancer, neurological problems, childhood developmental issues, cardiovascular disease, kidney and liver failure [471]. The maximum permissible limit recommended by WHO, USA for nickel copper and zinc are 0.2 mg/L, 2 mg/L and 5 mg/L. As a result, it is crucial to figure out how to get heavy metals out of the aqueous phase. Adsorption of heavy metals from wastewater has been investigated by using various adsorbents [472]. Preparation of organic waste adsorbent is more expensive than the inorganic adsorbents. Montmorillonite is a 2:1 mineral composed of one octahedral

sheet and two silica sheets arranged in a layer. It is a significant component of bentonites. These layers are held together by the Van der Waals forces. Water quickly penetrates these layers due to the weak forces, enabling cations to balance [473]. Bentonite is a smectite-group clay mineral found in nature. It has a broad active surface area, distinct hydration properties and strong cation exchange abilities. It is less expensive, widely available and effective against a wide range of impurities and metal ions. Due to these properties, bentonite clay is an excellent option for the heavy metal ion removal from bulk solutions [474], [475]. The ability of bentonite to adsorb cations is one of its valuable properties. Bentonite clay has been used as a heavy metal adsorbent in number of studies [206], [462], [472], [475], [476]. Adsorption takes place in soil when solution components cling to the surface of soil particles. This process is influenced by the inorganic and organic components of the soil's surface, as well as by related environmental conditions. Soil particles can include a wide variety of compounds, including soil components, plant nutrients, surfactants, insecticides and environmental pollutants found in soil solutions. Soils are amphoteric, with a broad spectrum of negative and positive charge and magnitude [179]. Soils maintain a steady negative charge due to structural flaws caused by ion replacements or site vacancies in crystalline clay minerals and non-crystalline hydrous oxides of silica, iron and aluminium [180]. Cations are adsorbed explicitly or non-specifically by inorganic and organic constituents of soils in terrestrial environment [181]. Due to the intrinsic structure and properties such as smaller ionic dimension and load, Zn^{2+} is heavily absorbed by soils. The highest adsorption potential is found in Zn^{2+} ion, which has the smallest ionic radius [182]. It was further observed by Akay and Doulati, 2012 [182] that clay rich soils have higher absorption capacity.Thus, moulds were prepared in this study by using bentonite clay and the soil obtained from the Samne ghat of Varanasi, India. The mould was tested for its ability to adsorb Cu^{2+}, Ni^{2+} and Zn^{2+} ions. In order to establish this, the mould was first physico-chemically characterized, followed by optimization study, isotherm, kinetic and thermodynamic modelling of adsorption data. Furthermore, dimensionless numbers were calculated to deduce the rate controlling step in this study. Additionally, ANN tool of MATLAB has been used to compare the experimental result with the predicted outcome

like other researchers [477], [478].

7.2 The Ganga River Bank (Ghat) in Varanasi

The sacred value is attached to the River Ganga in India, the riverfront is the city's most recognizable feature [479]. The riverfront, or the point at which the river meets the land, is defined as ghats. Varanasi has a humid subtropical climate with significant temperature difference between summer and winter. The basin's annual average rainfall ranges from 39 to 200 cm, with an average of 110 cm. 80% of rainfall occurs during the monsoon season, which runs from June to October. Due to the large temporal variations in precipitation throughout the year, the river's flow characteristics vary significantly [479]. According to the study [480], down-stream sampling stations had elevated concentrations of all heavy metals (Cd, Cr, Cu, Ni, and Pb). The primary sources of these elements in the atmosphere are emissions from adjacent urban and industrial areas. Vehicle emissions are the primary source of urban particulate matter. Resuspension of land-deposited particulate could provide additional evidence for heavy metal loading. The levels of Cd, Ni, and Pb at real time stations exceed the internationally recommended (WHO) maximum permissible concentrations [480]. Samne Ghat was one of the sites from which samples were collected. The only rationale for selecting Samne ghat is its high population density, which contributes to water contamination by the discharge of untreated industrial and domestic waste into bodies of water. Pollutants are emitted from residences and surrounding industrial units.

7.3 Results and Discussion

7.3.1 Physicochemical Characterization

7.3.1.1 SEM-EDS

Figures 7.1a and 7.1b depicts a SEM micrograph of mould before and after adsorption. It showed that the surface structure of mould was slack and porous, with a high specific surface area and sufficient adsorption zone. As a result, it was expected to have a high

adsorption capacity.

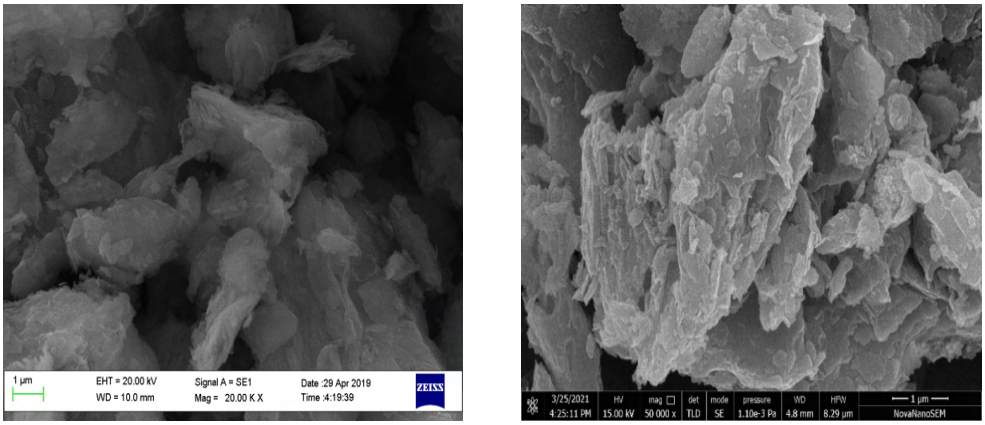

(a) **(b)**

Figure 7.1: (a) SEM of unloaded mould and (b) SEM of metal ions-loaded mould

Prior to adsorption, the surface has irregularities (Figure 7.1a) that aid in increasing surface area. As demonstrated in Figure 7.1b, the surface of the mould became saturated after metal ion adsorption. The surface of mould has schistose structures, which are preferable for the adsorption of Ni^{2+}, Cu^{2+} and Zn^{2+} ions [206], [481] (Figure 7.1b).
Schistosity is described as geological foliation (metamorphic layering) with medium to large grained flakes in a preferred sheet-like orientation [482]. Bentonite has a typical layered and puffy structure, which provides a framework for the adsorption [480]. Tahir et al., 2013 [483] also reported saturation of the surface active sites while removing reactive dyes using bentonite clay which was similar to present investigation.

The EDX spectra of the prepared mould is depicted in Figures 7.2 and 7.3.

The spectra of peaks corresponding to the elements potassium (K), oxygen (O), iron (Fe), magnesium (Mg), aluminium (Al), and silicon (Si) were observed in Figure 7.2. Chang et al., 2020 [206] recorded C, O, Na, Mg, Al, Si, Ca, Fe, S, and K during the adsorption of Cu^{2+} and Ni^{2+} ions on bentonite and bentonite/GO composites. Chang et al., 2020 [206] analyzed that bentonite lacked potassium and sulphur, but these elements were present in the Bentonite/GO composite. The disparity in the results of Cheng et al., 2015 [206] with the present work was due to different procedures of preparing the mould that altered the elemental composition. Sodium, magnesium, aluminium, silicon, calcium, and iron were

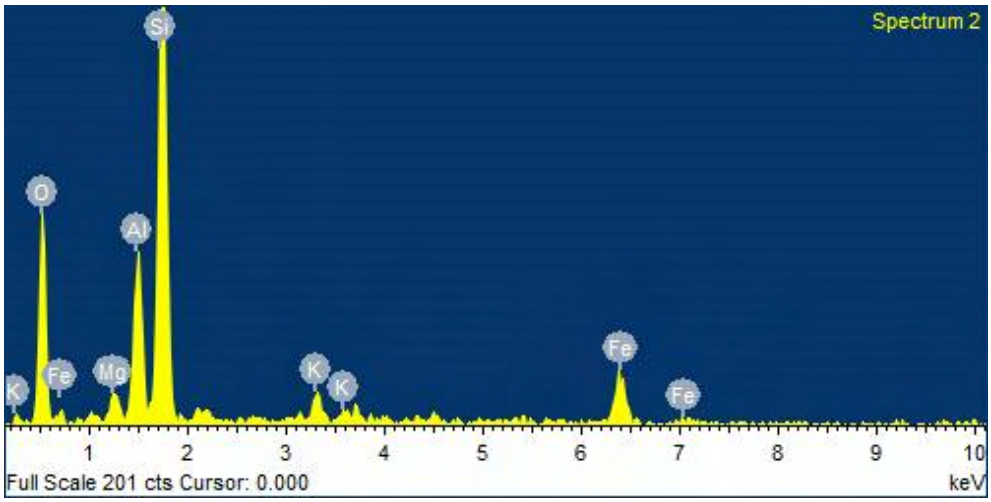

Figure 7.2: EDX of mould before adsorption

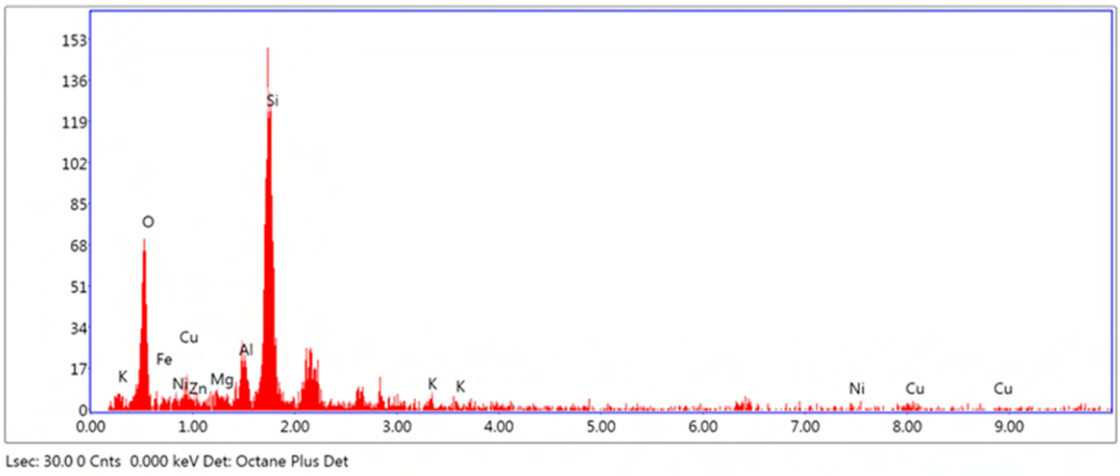

Figure 7.3: EDX of mould after adsorption of ternary metal ions

formed from the minerals albite, magnesia, aluminium oxide, silicon dioxide, wollastonite and iron in the tetrahedral and octahedral crystal structures of bentonite [206]. Hebbar et al., 2018 [480] reported that the primary constituents in bentonite clay are silicon (Si), aluminium (Al), and oxygen (O). These results were similar to the results obtained in present work. Figure 7.3 further validates the adsorption of Ni^{2+}, Cu^{2+} and Zn^{2+} ions.

7.3.1.2 FTIR

Figure 7.4 depicts the mould's FTIR spectra before and after adsorption. The absorption band at 3438.89 cm^{-1} is due to stretching vibrations of O-H groups and is associated with alcohol and phenolic compounds [267]. The peak at 1629.78 cm^{-1} was responsible for the water molecule's O-H bonds bending within the silicate matrix [206]. The peaks

at 1036.19 cm^{-1} and 777.77 cm^{-1} are induced by stretching vibrations of Si-O-Si, Si-O-Al and Al-O on tetrahedral and octahedral sheets [206]. The presence of a band at 777.77 cm^{-1} as a result of Al-Mg-OH stretching implies the presence of quartz, which was also supported by X-ray diffraction result [484]. The weak and medium sharp bands (693.22 cm^{-1} and 476.68 cm^{-1}) were due to Si-O stretching, Si-O-Al bending and Si-O-Si stretching, respectively [267]. Similar bands of Si-O-Si stretching at 463 cm^{-1}, stretching and bending vibrations of OH^- at 3426 cm^{-1} and 1637 cm^{-1} were reported by El-Enein et al., 2020 [54] during adsorption of some metals using nano-bentonite. Following the adsorption of metal ions, a shift in frequency was observed, as shown in Table 7.1.

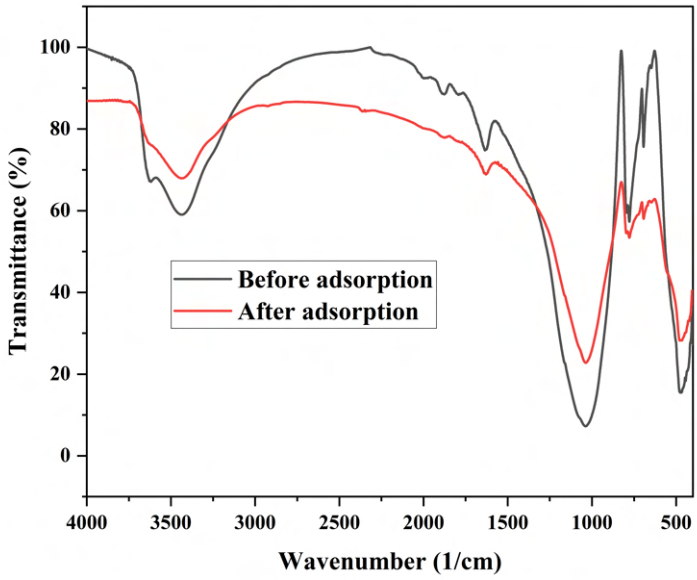

Figure 7.4: FTIR spectrum of mould before and after adsorption of ternary metal ions

The shift in the spectra of the mould before and after metal ion adsorption was seen in the FTIR spectrum (Figure 7.4). The transmittance rose after metal ion adsorption (Figure 7.4), and the intensity of few characteristic peaks was strengthened, while some characteristic peaks were displaced. The peak of the bentonite at 3625.71 cm^{-1} related to Al–O–H stretch was shifted to 3636.38 cm^{-1}, and the peaks of the stretching and bending vibration H–O–H groups at 3438.89 cm^{-1} and 1629.78 cm^{-1} were shifted to 3436.90 cm^{-1} and 1635.15 cm^{-1}, respectively. The Al–O–H and H–O–H groups of mould was involved in the metal ion adsorption [485].

Table 7.1: FTIR band positions of the prepared mould before and after adsorption

Frequency (1/cm) (Before adsorption)	Frequency (1/cm) (After adsorption)	Appearance	Group	Compound class
3625.71	3636.38	Narrow	Al-O-H stretching	Octahedral
3438.89	3436.90	Broad	H-O-H stretching	Absorbed water
1629.78	1635.15	Medium	H-O-H bending	Physisorbed
1036.19	1038.89	Strong	Si-O-Si stretching	Tetrahedral
777.77	777.90	Weak broad	Si-O-Al stretching Al-Mg-OH stretching	Alkyne, Quartz, Mono-substituted
693.22	693.56	Weak sharp	Si-O stretching Si-O-Al bending	Alkynes, Benzene derivative
476.68	468.87	Medium sharp	Si-O-Si stretching	Silicon monoxide

7.3.1.3 XRD

Figure 7.5 depicts the mould's X-ray diffraction spectrum. Before adsorption, the absorption peaks were found at 2θ of 8.94°, 19.81°, 25.97°, 26.71°, 28.00°, 36.62°, 39.47°, 39.93°, 42.51° and 50.20° while after adsorption, peak position changes to 8.99°, 21.02°, 21.02°, 26.78°, 27.09°, 36.68°, 36.68°, 42.58° and 50.27° (Figure 7.5). The maximum peak appeared at 26.68° and 26.84° before and after adsorption, respectively. The maximum crystallite size appeared at 26.17º. The average crystallite size (Dp) was 41.29 nm and 36.97 nm before and after adsorption, respectively. The explanation for this is the shift in diffraction peaks, caused due to changes in lattice parameters. The XRD pattern shows the presence of montmorillonite (M) [486], illite (I) [487], quartz (Q) and feldspar (F) [488], [489]. The peaks, similar to the present study were found by Burham and Sayed,

2016 [267] while studying adsorption behaviour of metal ions onto Egyptian bentonite clay. Thus, confirmed the presence of bentonite in the mould.

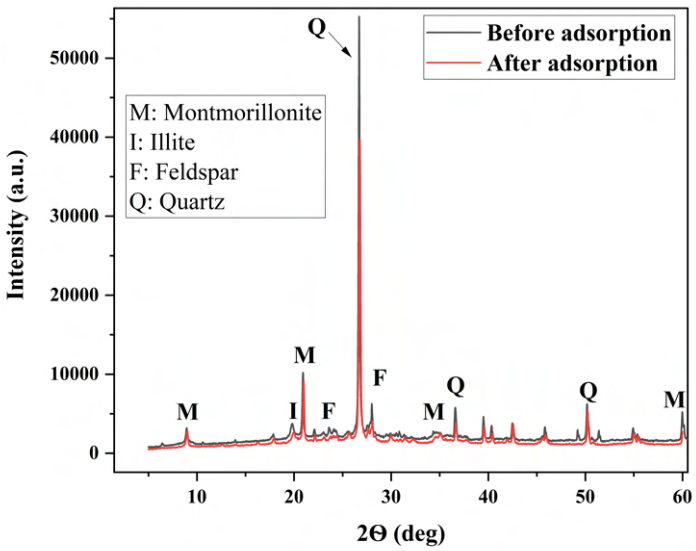

Figure 7.5: XRD of mould before and after adsorption of ternary metal ions

The XRD graph of mould revealed that the substance is partly amorphous and finds application as an adsorbent [490]. It was also observed that the mould is less crystalline (43.35%) or more amorphous (56.65%). This helps in enhancing the adsorption efficiency of adsorbent. Scherrer equation [196] was used to calculate the crystallite size of the mould and the results are shown in Table 7.2.

Table 7.2: Calculated values of D and FWHM for the corresponding absorption peaks

(a) Before adsorption

2θ	FWHM	D (nm)
8.94	0.17	46.25
19.82	0.51	15.67
20.92	0.17	46.41
26.71	0.16	50.77
36.62	0.21	39.65
39.53	0.19	45.41
40.35	0.19	44.28
42.50	0.20	43.05
50.20	0.22	40.12

(b) After adsorption

2θ	FWHM	D (nm)
8.95	0.28	28.46
19.82	0.44	18.32
20.95	0.16	50.79
26.72	0.16	51.95
36.62	0.27	30.76
39.54	0.22	37.77
40.38	0.24	35.56
42.54	0.22	38.54
50.22	0.22	40.54

7.3.1.4 Proximate Analysis

The proximate analysis of the mould was performed in accordance with the ASTM D 121 standard [491] (Table 7.3).

Table 7.3: Proximate analysis of mould

Ash	Moisture	Volatime matter
4.5	0.49	95.01

The mould was found to have a low moisture and ash, and a high volatile matter content based on the proximate analysis. Dutta et al., 2017 [492] observed similar kind of results. Additionally, Eltawil et al., 2015 [493] reported that higher volatile matter leads to higher extent of porosity with enlarged pore structure. It means that the mould developed in this study has far more porosity to aid in the adsorption of target metal ions.

7.3.1.5 TGA

The mould was analyzed using TGA at temperatures ranging from 22 to 1000°C in a nitrogen atmosphere (Shimadzu, model TGA-50H, heating rate 10°/min). TGA and derivative thermogravimetry (DTG) curves for mould are shown in Figure 7.6. The mould had endothermic peaks near 200°C, indicating the presence of both free and absorbed water that was removed during dehydration reactions [257], [494]. Endothermic peaks close to 200°C have been also linked to the presence of water coordinated with Ca^{2+} and Mg^{2+} ions [257].

Furthermore, the organic matter in mould decomposed between 200°C and 600°C [495]. The dehydroxylation of the clay minerals and lattice water contained in the mould with other external components present in the clay minerals, resulted in a small weight loss in the mould in the temperature range of 370 to 900°C [496], [497]. Since the mould contains very little inorganic and organic carbon, only a small amount of mass loss was apparent in the Figure 7.6 [495]. However, increasing the temperature further from 890 to 1000°C led to no mass loss, indicating that the mould was thermo-stable [495].

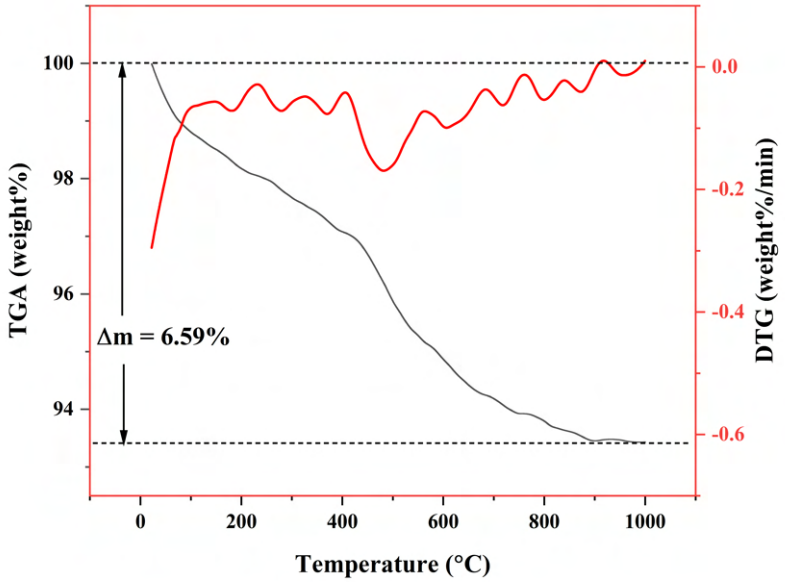

Figure 7.6: TGA and DTG curves of mould

7.3.2 Adsorption Dynamics

The value of dimensionless numbers φ, λ and N_k as well as film and pore diffusivity coefficients are shown in Table 7.4. The data shows that pore diffusion is the most prominent adsorption mechanism, with values ranging from 10^{-11} to 10^{-13}. Film diffusion, on the other hand, is not the process involved because the values are not in the range of 10^{-6} to 10^{-8}.

The value of N_k was between 10^{-4} and 10^{-3} which interpreted that adsorption dynamics was transfer-controlled as the main mechanism behind adsorption. The value of φ and λ indicated that the mould surface was covered in significant quantities with reduced surface tension [212].

Table 7.4: Dimensionless numbers and diffusivity coefficients for the adsorption of metal ions in mould

Dimensionless numbers	φ	λ	N_k	D_P (cm^2sec^{-1})	D_F (cm^2sec^{-1})
Cu^{2+}	133.98	3.05×10^{-5}	3.06×10^{-3}	1.45×10^{-11}	1.01×10^{-12}
Ni^{2+}	133.75	7.09×10^{-5}	3.07×10^{-3}	1.05×10^{-12}	5.22×10^{-11}
Zn^{2+}	133.27	1.41×10^{-4}	3.08×10^{-3}	1.17×10^{-12}	2.9×10^{-11}

7.3.3 ANN Modeling

pH, adsorbate concentration, contact time and temperature were provided as network inputs. The back-propagation technique with the L-M algorithm was used to predict output function. The network was trained until lesser number of epochs were obtained [235]. Thereafter, the network simulation was processed with the experimental data. The predictive output function was compared with the experimental results. Figure 7.7 shows the

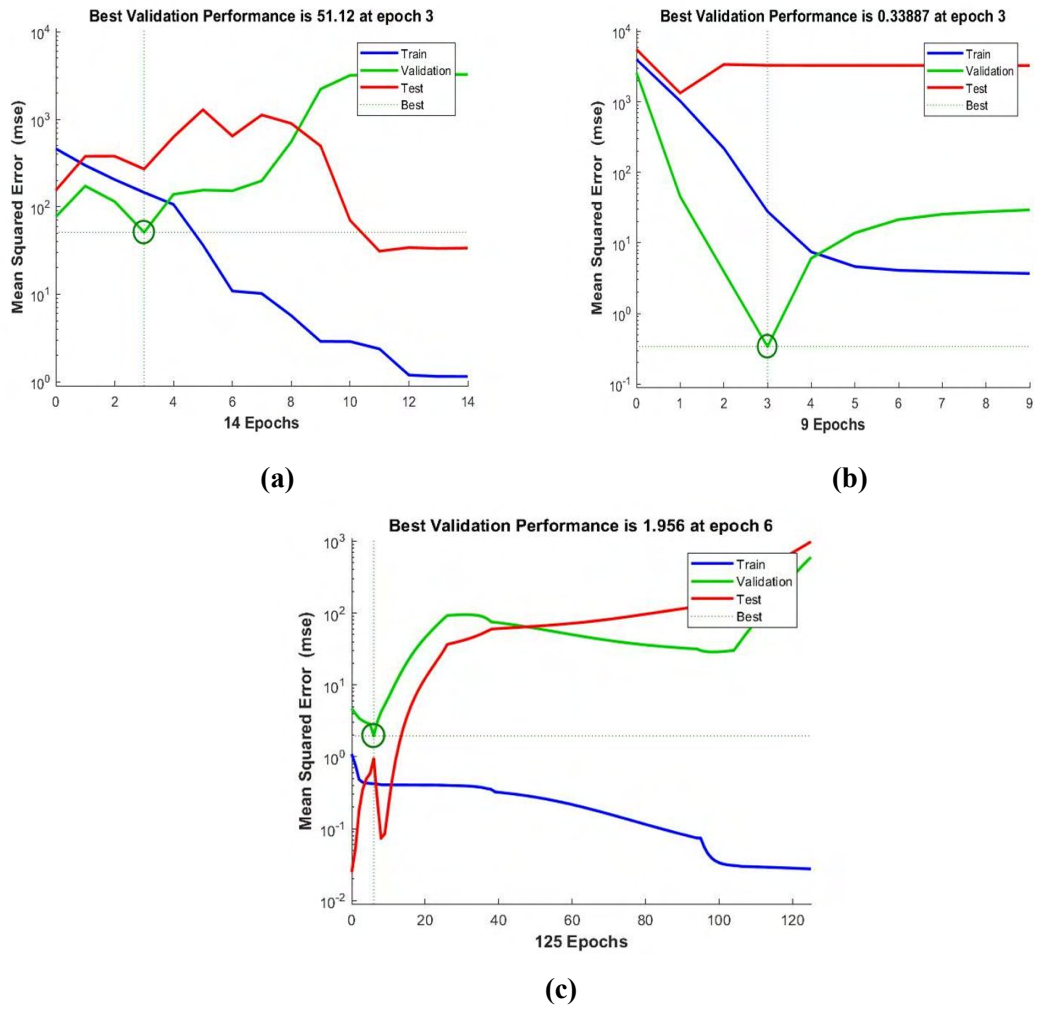

Figure 7.7: Performance between number of epochs and MSE for prediction of (a) Ni^{2+}, b) Cu^{2+} and (c) Zn^{2+} ions removal using mould as adsorbent

MSE of the ANN model obtained in training, testing and validation of data. The lowest MSE (encircled point) was recorded during training, testing and validation of data by L-M algorithm. Similar results were found by Yildiz, 2018 [232] with best validation performance 0.0011846 at epochs 27 for Ni^{2+} ions.

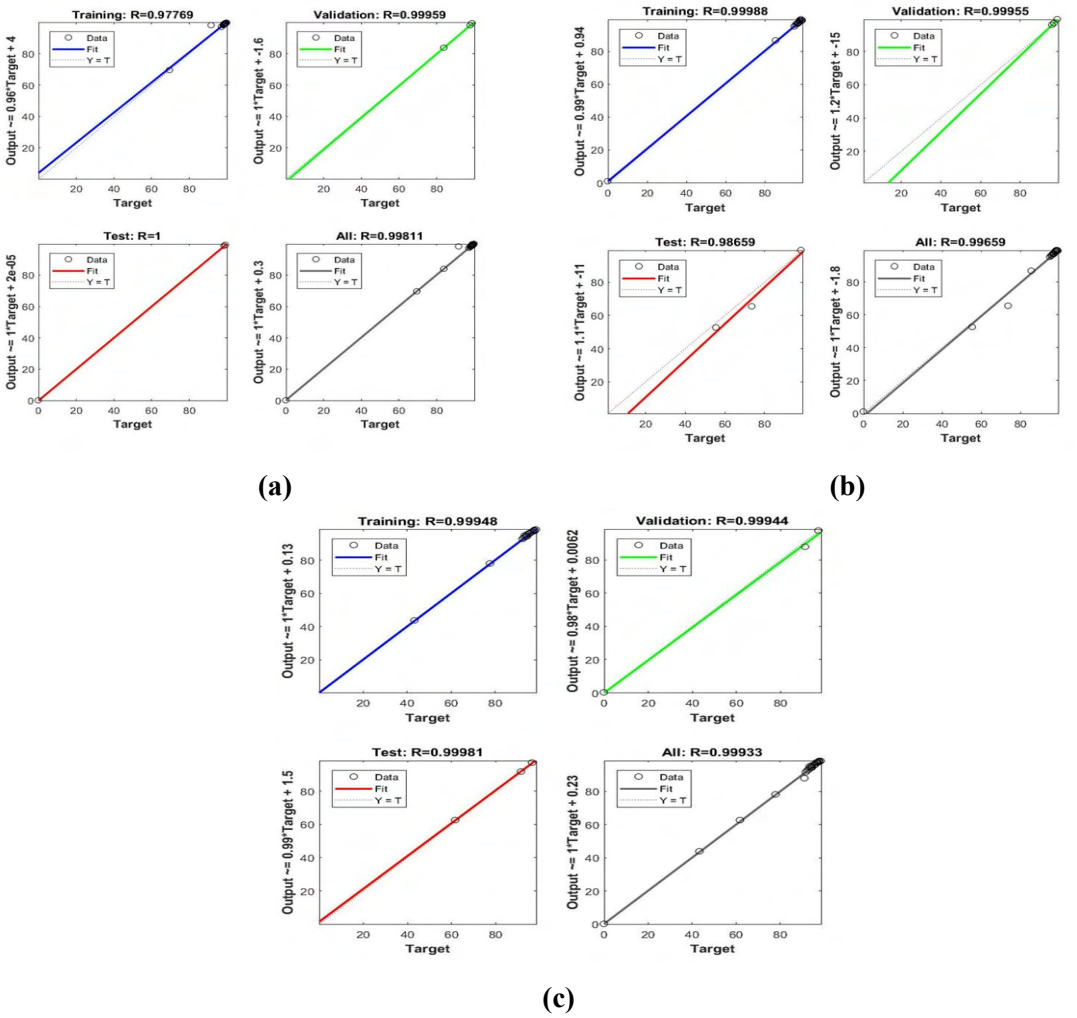

Figure 7.8: Regression plot for prediction of (a) Ni^{2+}, (b) Cu^{2+} and (c) Zn^{2+} ions removal using mould as adsorbent

Figure 7.8 shows regression between experimental and predicted values for the adsorption of Cu^{2+}, Ni^{2+} and Zn^{2+} ions on mould. The circles in the plot are experimental values and the colored lines show the predicted values derived from ANN models.

Both the experimental and theoretical values seemed to be in agreement with each other showing a high regression coefficient (R^2 value of 0.99) (Figure 7.8). Thus, in the present work, the L-M algorithm was concluded appropriate for predicting the output function with the lowest MSE at epoch (3, 3, 6 for Ni^{2+}, Cu^{2+} and Zn^{2+} ions) coupled and highest validation performance in ten neurons at 51.12, 0.33887 and 1.956 for Ni^{2+}, Cu^{2+} and Zn^{2+} ions, respectively (Figure 7.7).

The results also showed a small deviation of 0.29% for Ni^{2+}, 0.28% for Cu^{2+} and 0.0046% for Zn^{2+} ions between the experimental and predicted values (Figure 7.9). This further

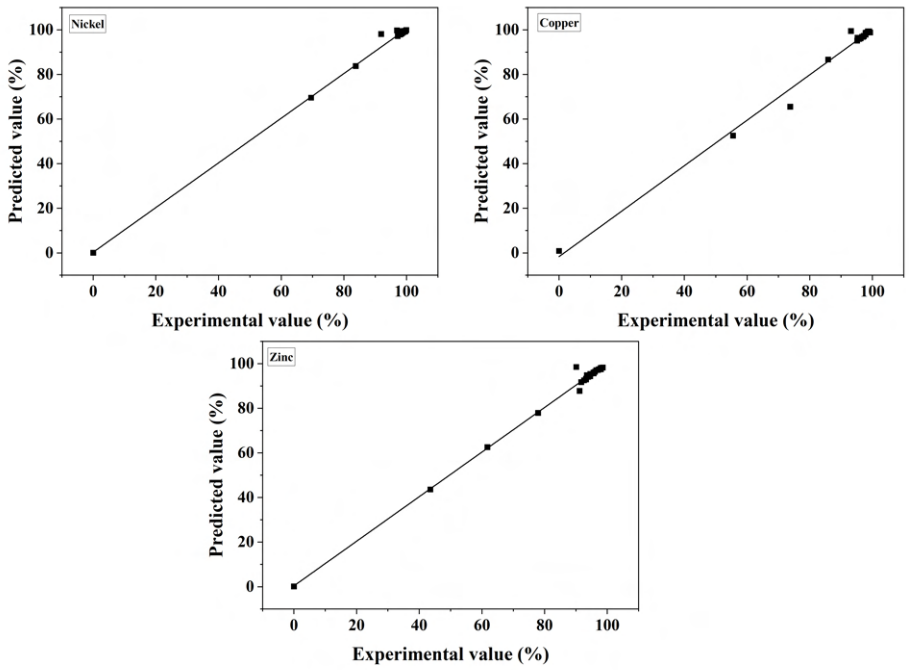

Figure 7.9: Correlation plot for the experimental and ANN predicted values for ternary metal ions removal using mould as adsorbent

showed the suitability of L-M algorithm in the present work. ANN were also used for modeling Cu^{2+} adsorption on zeolite surface [273]. Adsorbent dose, contact time and pH were given as input for simulating experimental results. The authors observed that the L-M back-propagation training function with ten neurons in the hidden layer were the most efficient network, similar to the present study. Similarly, Yildiz, 2018 [232] applied ANN in the adsorption of Ni^{2+} from aqueous solution on peanut shell surface and found a high regression coefficient ((R) training (0.99), test (0.97) and validation (0.99)) between experimental and predicted values.

7.3.4 Adsorption Kinetics

As illustrated in Figures 7.10, 7.11 and 7.12, PFO, PSO, and IPD kinetic models in linear form are evaluated to depict the adsorption of Ni^{2+}, Cu^{2+} and Zn^{2+} ions using mould. Table 7.5 summarizes the kinetic parameters from the PFO, PSO and IPD models. In the present study, PSO model with a high R^2 values provided a better explanation for the adsorption of Ni^{2+}, Cu^{2+} and Zn^{2+} ions on mould. The adsorption of these metal ions

followed heterogeneous diffusion model.

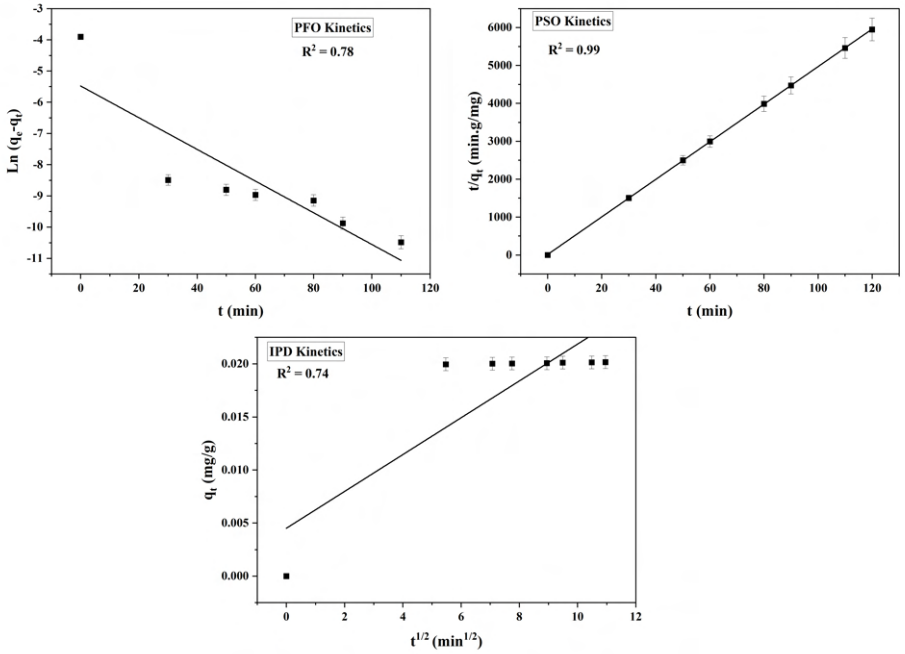

Figure 7.10: Adsorption kinetics for Ni^{2+} ions using mould as adsorbent

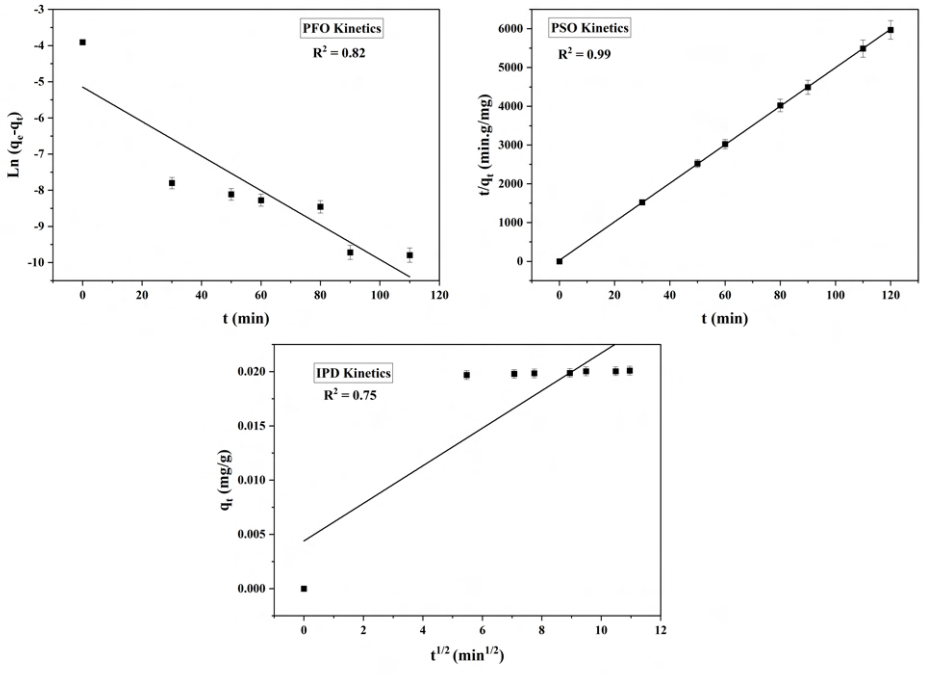

Figure 7.11: Adsorption kinetics for Cu^{2+} ions using mould as adsorbent

Similarly, He et al., 2020 [498] conducted research to elucidate the adsorption kinetic mechanism during the adsorption of heavy metal ions on soil and discovered that PSO kinetic model ($R^2 = 0.99$) was best fitted into their data, followed by intraparticle diffusion

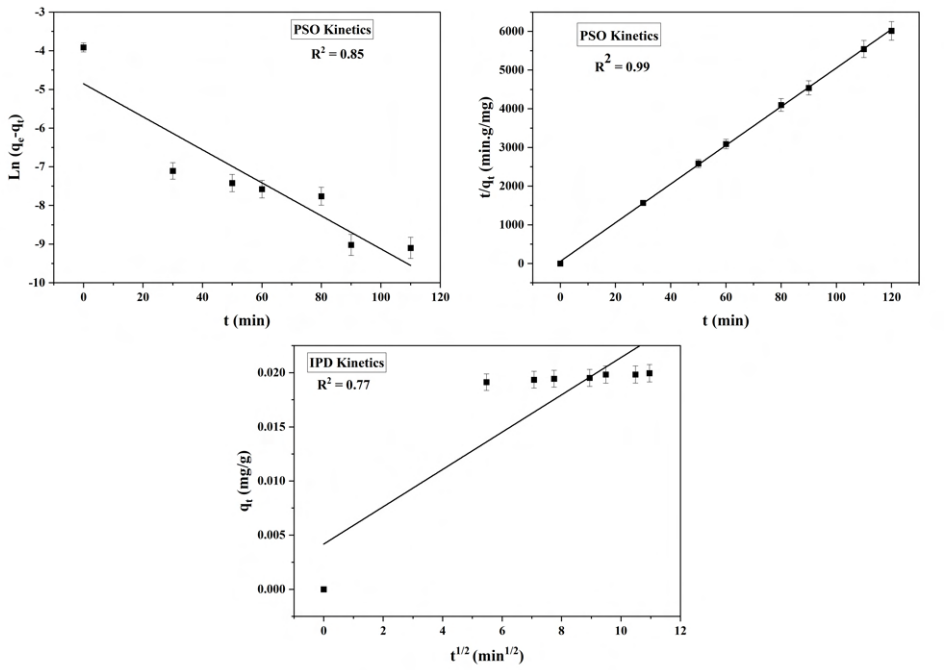

Figure 7.12: Adsorption kinetics for Zn^{2+} ions using mould as adsorbent

(R^2 = 0.95). Mohamed et al., 2020 [473] studied the kinetics of copper and zinc ions adsorption on the clay and reported that PSO model (R^2 = 0.99) was the best fitted model and adsorption was controlled by chemisorption mechanism.

Table 7.5: Kinetic parameters

Kinetic Parameter		PFO		PSO		IPD	
		q_e (mg/g)	k_1 min^{-1}	q_e (mg/g)	k_2 (g/mg. min)	k_p (mg/g. min)	C (mg/g)
Value	Cu^{2+}	0.0042	0.05	0.0202	192.79	0.00174	0.0054
	Ni^{2+}	0.0058	0.047	0.0201	95.14	0.00173	0.0050
	Zn^{2+}	0.0078	0.042	0.0200	46.60	0.00172	0.0043
R^2	Cu^{2+}	0.78		0.99		0.74	
	Ni^{2+}	0.82		0.99		0.75	
	Zn^{2+}	0.85		0.99		0.77	

7.3.5 Adsorption Isotherm

In the present study, Langmuir, Freundlich and D-R isotherm are evaluated to depict the adsorption of Ni^{2+}, Cu^{2+} and Zn^{2+} ions using mould (Figures 7.13, 7.14, 7.15 and Table 7.6).

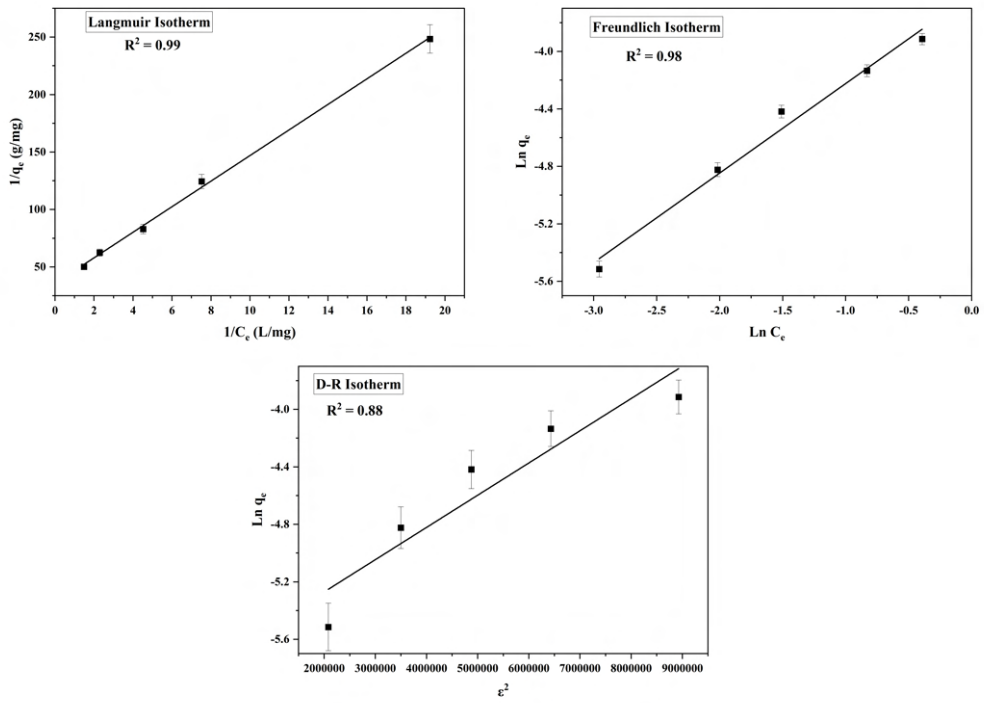

Figure 7.13: Adsorption isotherm for Ni^{2+} ions

Table 7.6: Isotherm parameters

Isotherm		**Langmuir**		**Freundlich**		**D-R**	
Parameter		**q_m (mg/g)**	**K_L (L/mg)**	**n**	**K_F (L/mg)**	**E (J/mol)**	**q_m (mg/g)**
Value	**Cu^{2+}**	0.086	0.31	1.61	0.03	1.507	0.0032
	Ni^{2+}	0.045	0.61	1.62	0.02	0.916	0.0033
	Zn^{2+}	0.021	1.16	1.64	0.01	0.531	0.0035
R^2	**Cu^{2+}**	0.99		0.99		0.88	
	Ni^{2+}	0.99		0.99		0.83	
	Zn^{2+}	0.99		0.95		0.82	

The results demonstrated explicitly that the presence of other metal ions in the system

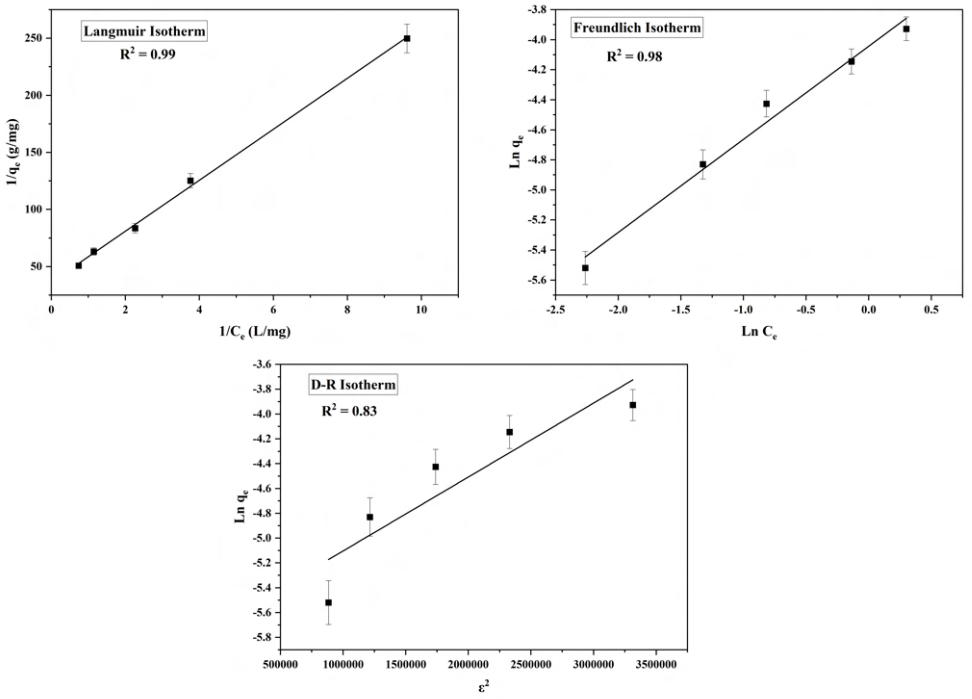

Figure 7.14: Adsorption isotherm for Cu^{2+} ions

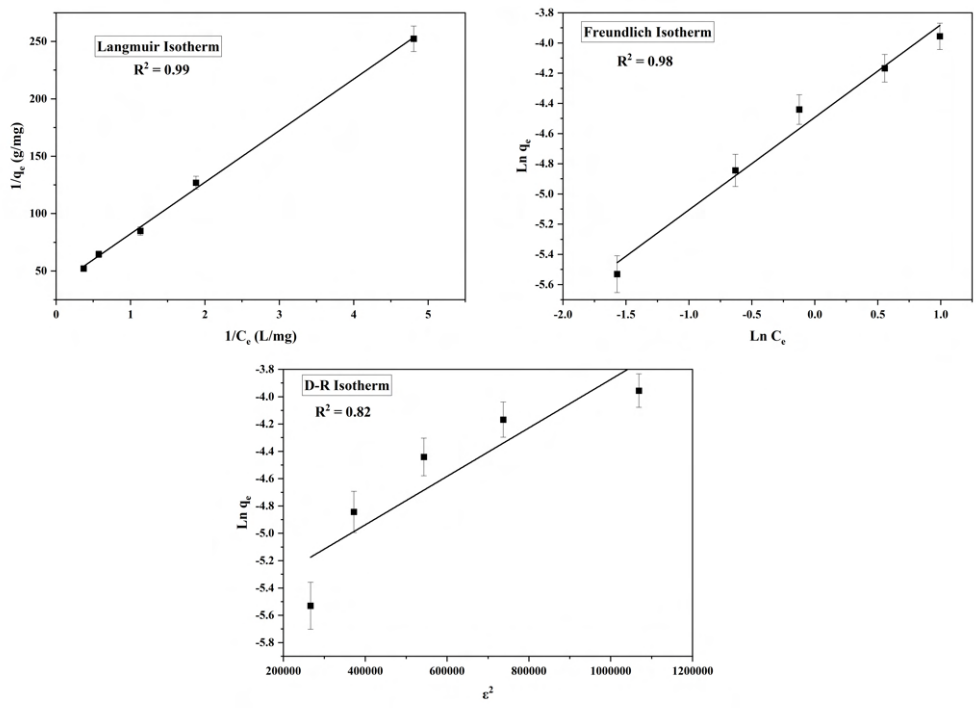

Figure 7.15: Adsorption isotherm for Zn^{2+} ions

reduced the overall adsorption potential in the tertiary system. The maximum adsorption capacities of Langmuir for Ni^{2+}, Cu^{2+} and Zn^{2+} ions are 0.086 mg/g, 0.045 mg/g,

and 0.021 mg/g, respectively. The results indicated that the ability of mould to adsorb decreased in the order of Ni^{2+} > Cu^{2+} > Zn^{2+}. This was due to ion exchange in the adsorption of cations, a cation with a smaller hydration radius adsorbs more quickly due to its greater ability to attract electrons [499], [500]. The hydration radius is in order of Ni^{2+} (4.04) < Cu^{2+} (4.19) < Zn^{2+} (4.30) [501]. The order of sorption affinity observed here is consistent with ref. [502], [503].

Freundlich model also fitted to the experimental data well, but R^2 values were relatively lower than obtained for the Langmuir model. Although mould has a minimal sorption ability, the Freundlich isotherm was less appropriate for describing cation sorption on mould [504]. The adsorption intensity is expressed in terms of heterogeneity factor 'n'. The adsorption is preferable when n is between 1 to10. If n is less than one, the adsorption is negligible. In the present work, the values of n were in the range of 1 to 2 which showed the preferential adsorption of Ni^{2+}, Cu^{2+} and Zn^{2+} ions on mould.

Adsorption onto micro -porous solid materials and heterogeneous surfaces is explained by D-R isotherm. This isotherm has been frequently used to determine the presence of physical or chemical adsorption. The values of D-R isotherm parameters are summarized in Table 7.6. The q_{max} derived from Langmuir and D-R models are not identical. This was owing to the fact that the two models use different definitions of maximal adsorption capacity [476]. The lower R^2 values of D-R isotherm plots as compared to Langmuir and Freundlich plots reflected that the D-R model is less useful for depicting adsorption. The magnitudes of 'E' in this study are 1.507 kJ/mol for Ni^{2+} ions, 0.916 kJ/mol for Cu^{2+} ions, and 0.531 kJ/mol for Zn^{2+} ions, respectively. These 'E' values exhibited that the adsorption of metal ions on mould was physical in nature.

7.3.6 Thermodynamics Study

The slope and intercept values of the linear plot of ln K_d vs. 1/T were used to obtain the values of ΔH^o and ΔS^o, respectively (Figures 7.16, 7.17 and 7.18).

The ΔH^o parameter had a value of 15717.53, 17480.52 and 17422.32 kJ/mol and the ΔS^o parameter was found to be 25.86, 25.69 and 19.37 kJ/mol K for Ni^{2+}, Cu^{2+} and Zn^{2+} ions,

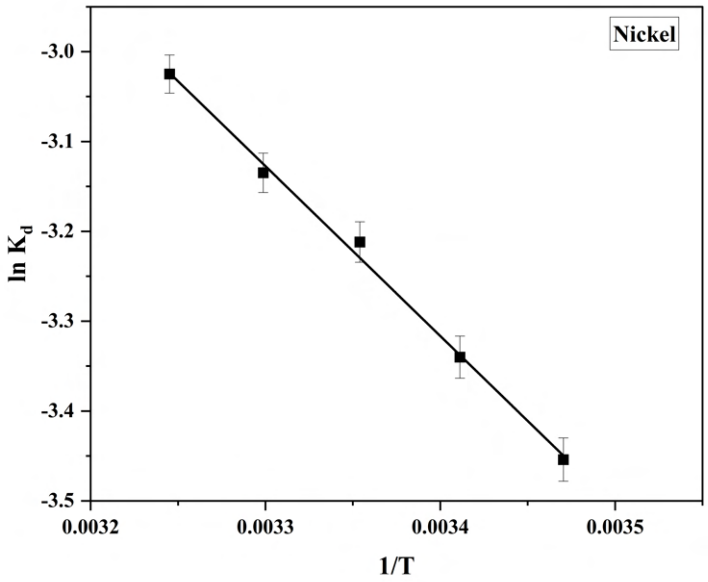

Figure 7.16: Plot of ln K_d vs 1/T for Ni^{2+} ions

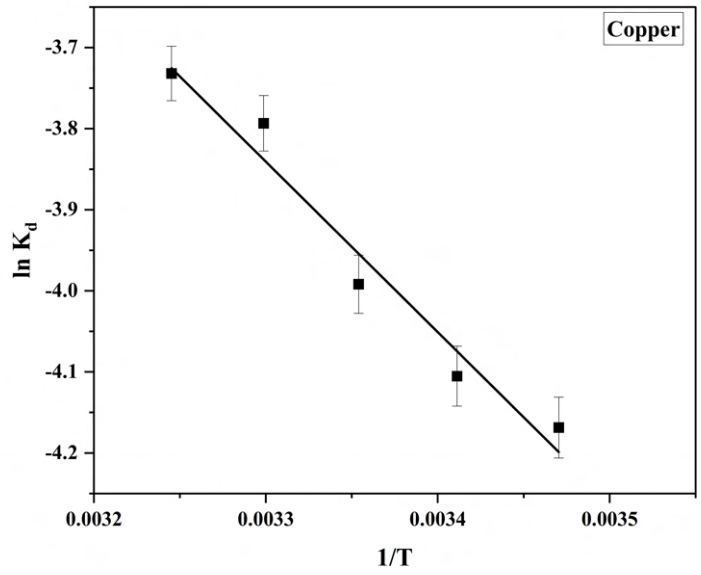

Figure 7.17: Plot of ln K_d vs 1/T for Cu^{2+} ions

respectively (Table 7.7). The enthalpy change is positive, indicating that the adsorption is endothermic, and the significant ΔH^o value suggests that there are strong contacts between the metal ions and the functional groups on the mould surface. The increase in randomness at the solid-liquid interface correlates to a positive entropy change value, and considerable changes in the internal structure of the sepiolite may occur as a result of the adsorption of Ni^{2+}, Cu^{2+} and Zn^{2+} ions on the mould [319]. ΔG^o was calculated for different temperatures (Table 7.7). The positive ΔG^o values suggested that the adsorption of Ni^{2+}, Cu^{2+} and

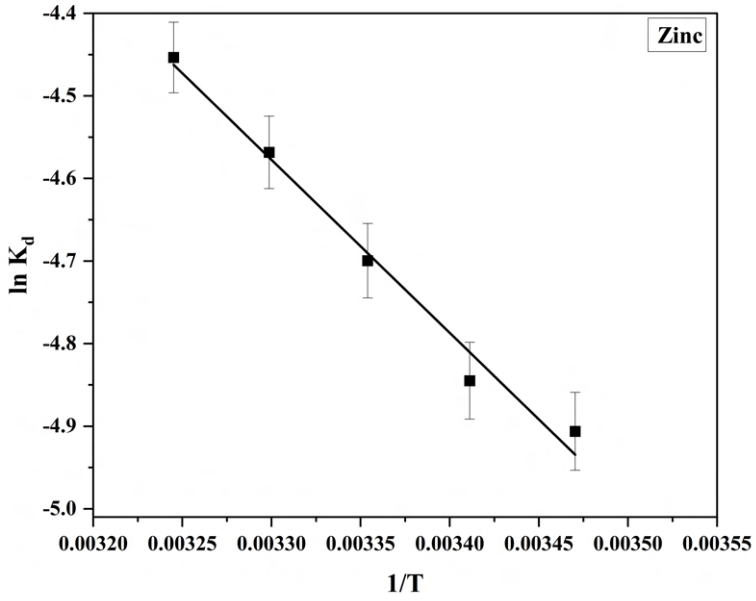

Figure 7.18: Plot of ln K_d vs 1/T for Zn^{2+} ions

Zn^{2+} ions on mould was thermodynamically non spontaneous [505]. This was further corroborated by the positive ΔH^o values observed for Ni^{2+}, Cu^{2+} and Zn^{2+} ion adsorption [506]. Similar observation were found by Asci and Berkan, 2010 [505] during removal of Cr (III) ions by using sepiolite and also by Ghibate et al., 2021 [507] while studying kinetics and thermodynamics of Rhodamine B adsorption onto pomegranate peel.

7.3.7 Optimization Study

7.3.7.1 Effect of pH

The effect of pH on adsorption of and Ni^{2+}, $Cu^{2+}$and Zn^{2+} is shown in Figure 7.19. The percentage adsorption was increased from 69.54 to 99.92%, 55.51 to 97.24% and 43.32 to 93.24% from pH 2 to 10 for Ni^{2+}, Cu^{2+} and Zn^{2+} ions, respectively. At low pH values, the hydrogen ions compete with the metal cation for the same active site and the minimal sorption at pH 2 may be attributed to the high concentration and mobility of H^+ ions in the liquid phase. The decrease in the percentage removal of metal ions at higher concentration of hydrogen ions indicated that the metal ion adsorption was mediated by ion-exchange mechanism [287]. In the present work, the optimum pH was taken as 6. Above pH 6, metals form insoluble hydroxide which results in precipitation rather than

Table 7.7: Thermodynamic parameters for ternary metal ions adsorption

Temperature (K)		Ni^{2+}	Cu^{2+}	Zn^{2+}
ΔG° (J/mol) (Experimental)	**288**	8266.97	10077.87	11840.39
	293	8137.68	9949.42	11743.53
	298	8008.40	9820.97	11646.67
	303	7879.12	9692.52	11549.81
	308	7749.84	9564.06	11452.95
ΔH° (J/mol K)		15717.53	17480.52	17422.32
ΔS° (kJ/mol)		25.86	25.69	19.37

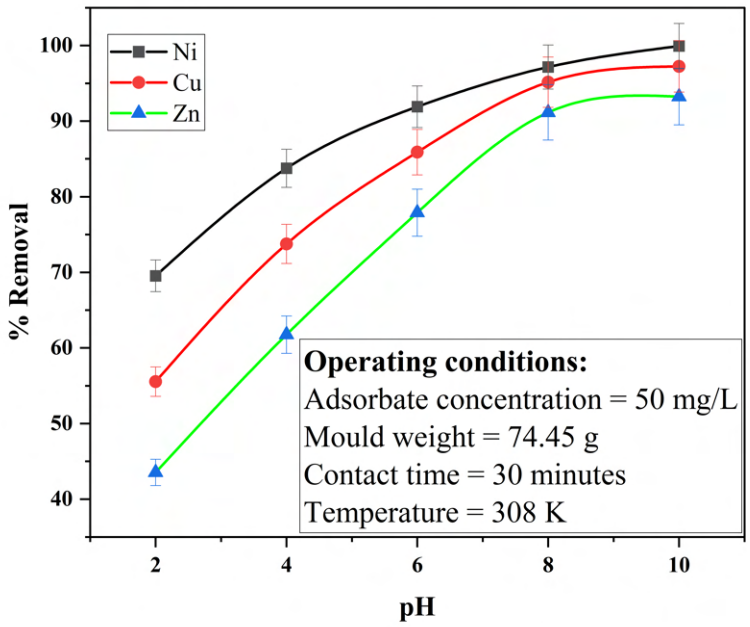

Figure 7.19: Effect of pH on % removal of ternary metal ions

adsorption [289], [290]. Hamdache et al., 2019 [313] studied removal of copper, nickel and zinc using bentonite clay in mono and multimetal system and found optimum pH of 5. At this pH range, H^+ ions leave the active sites of bentonite(deprotonation), and surface of

adsorbent became more negatively charged. This favors the positively charged metal ions to be adsorbed, resulting in enhancement in the metal ions removal. Similarly, Ghomri et al., 2013 [275] performed removal of copper, zinc and nickel by bentonite clay and found that high adsorption capacity were discovered between pH 3 and 5 for the bentonite which indicated high affinity for metal ions was predominant in this pH region.

7.3.7.2 Effect of Initial Concentration

The influence of the initial concentration of Ni^{2+}, Cu^{2+} and Zn^{2+} ions is demonstrated in Figure 7.20.

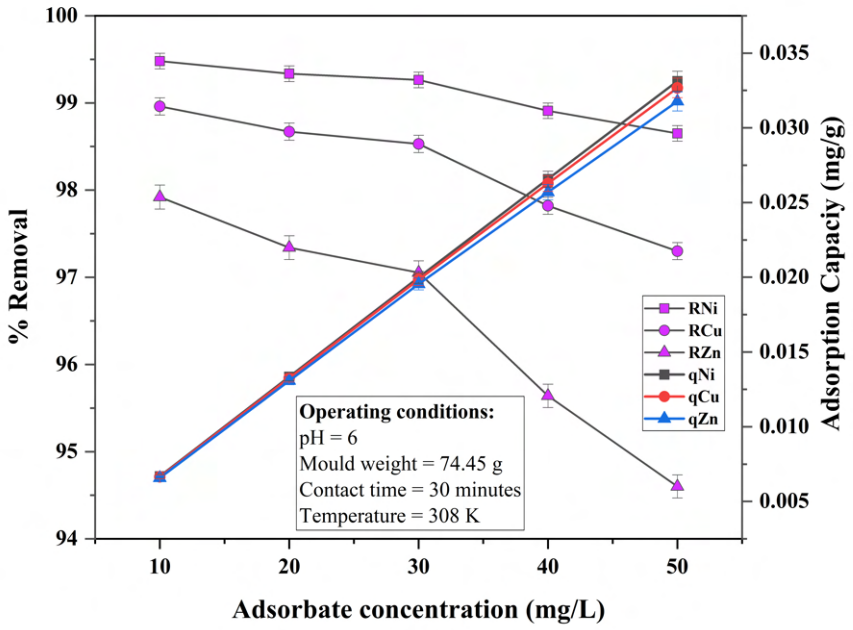

Figure 7.20: Effect of initial concentration on % removal of ternary metal ions and adsorption capacity of mould

It is obvious from Figure 7.20 that percentage removal declined from 98.96% to 97.30%, 99.48% to 98.65% and 97.92% to 94.60% for Cu^{2+}, Ni^{2+} and Zn^{2+} ions, respectively as the metal ions concentration increased from 10 to 50 mg/L. Such a reduction was due to a fixed number of active sites on the mould, and all active sites were entirely occupied at higher metal concentrations. The adsorption capacity of mould enhanced with an increase in the metal ion concentration. This increase was driven by increasing concentration gradient, a driving force for overcoming the mass transfer resistance between metal ions and the

solid phase. Tsai et al., 2016 [508] also obtained similar results with initial concentration of 10-200 mg/L during adsorption of zinc, lead, nickel and copper on chitosan-coated montmorillonite beads in single metal and multi metal system.

7.3.7.3 Effect of Temperature

The temperature effect on adsorption of Cu^{2+}, Ni^{2+} and Zn^{2} ions is shown in Figure 7.21.

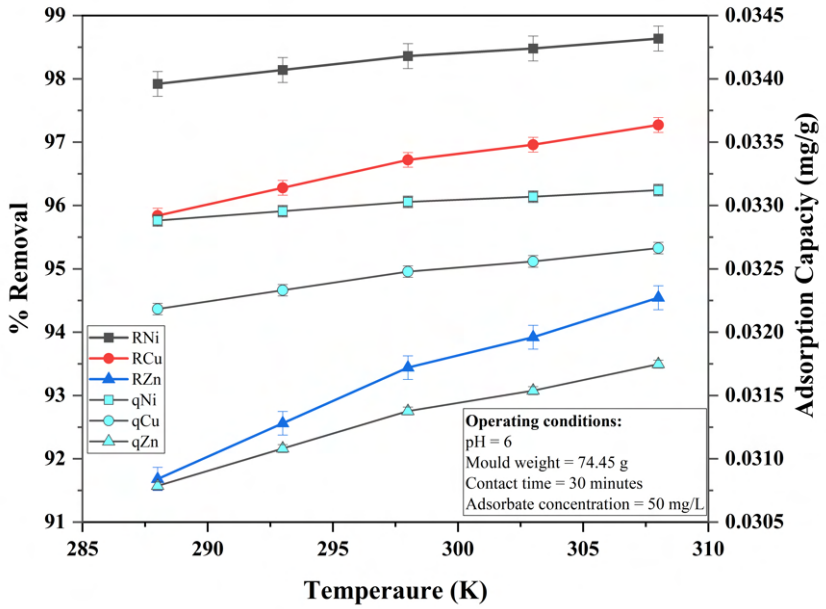

Figure 7.21: Effect of temperature on % removal of ternary metal ions and adsorption capacity of mould

It is evident from Figure 7.21 that the adsorption of metal ions improved with an increase in temperature from 288 to 308 K. This showed that the adsorption of Cu^{2+}, Ni^{2+} and Zn^{2+} was endothermic. Increased adsorption at higher temperature was attributed to generation of more active surface sites on the mould and reduced boundary thickness around the composite which reduced the mass transfer resistance in the boundary layer [297]. Similar to the present study, Ghomri et al., 2013 [275] experimented with temperature from 15 to 40°C for finding optimum temperature for removing copper, cobalt, nickel and zinc using natural bentonite and found that the increase in adsorption with temperature might be attributed to either a rise in the number of active surface sites accessible for metal ion adsorption or an increase in the surface area available. In the research done by

Hamdache et al., 2019 [313], a constant temperature of 293 K was taken for removal of copper, zinc and nickel by using bentonite clay.

7.3.7.4 Effect of Contact Time

The effect of contact time on adsorption of ternary metal ions is shown in Figure 7.22.

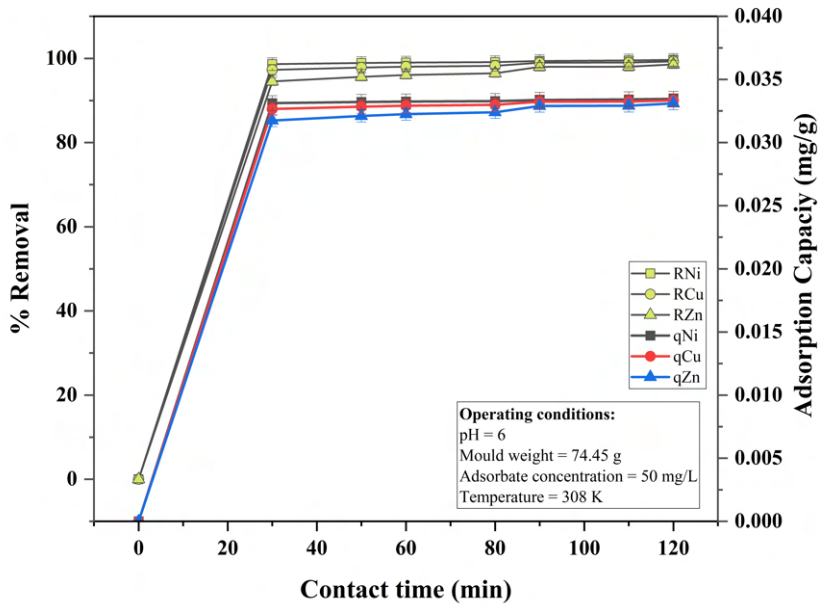

Figure 7.22: Effect of contact time on % removal and adsorption capacity of mould

The adsorption of ternary metal ions on mould increased with escalation of contact time up to 30 minutes for Cu^{2+}, Ni^{2+} and Zn^{2+} ions. Thereafter, there were no significant increase in the removal of these metal ions. Significant removal of Cu^{2+}, Ni^{2+} and Zn^{2+} ions occurred in mentioned time and the order of adsorption of metal ions was $Ni^{2+} > Cu^{2+} > Zn^{2+}$.

The disparity in chemical affinity and mould ion exchange ability for the specific chemical group led to variations in the removal of ternary metal ions under similar experimental conditions. Similarly, Ghomri et al., 2013 [275] found an equilibrium contact time of 60 minutes for copper ions and 150 minutes for cobalt, nickel and zinc ions during removal of copper, cobalt, nickel and zinc by using natural bentonite. Tsai et al., 2015 [508] performed adsorption of copper, lead, nickel and zinc on chitosan-coated montmorillonite beads in range of 30-300 minutes and maximum removal was found in the first 30 minutes, similar

to present work.

7.4 Adsorption mechanism for mould

Many intermolecular interactions between solid phase and solute can be examined by referring to how matter accumulates at the solid/water interface in two dimensions [509]. It includes reactions between inner-sphere surfaces complex of metal ions and functional groups on the surfaces, and electrostatic interactions, where the latter form complexes with the metal ions away from the surface. Most heavy metal adsorption pathways can be broken down into specific and nonspecific, with the former being more selective and less reversible processes (chemisorbed) and the latter including weaker, less selective outer-sphere complexes (or ion exchange) [510]. During non-specific adsorption, cations from the pores are exchanged with cations on the surface, whereas during specific adsorption, heavy metal ions bind strongly and irreversibly with organic matter and variable charge minerals. Cation exchange is an outer-sphere complexation in which metals and charged soil surfaces have only weak covalent bonds. It's a diffusion-controlled electrostatic interaction, therefore it occurs rapidly and can be reversible in nature [511]. A silanol group, an inorganic hydroxyl group, or an organic functional group can all be used as surface functionalities. The adsorbing cation forms a direct bond with the surface atoms using an inner sphere mechanism. As a result, the surface characteristics and metal composition of the adsorption site affect the adsorption potential [301]. For a metal cation M and a mould surface S (Eq. 7.1), the reactions are equivalent to heavy metal ion hydrolysis and are pH-dependent.

$$S - OH + M^{2+} + H_2O \leftrightarrow S - O - MOH_2^+ + H^+ \tag{7.1}$$

Hydrous oxide minerals can be found in mould. They have hydroxyl groups on the surface that can contribute protons to the surrounding solution in exchange for metal ions. As a result, the pH affects metal ion adsorption on these surfaces. Aluminosilicates (clay minerals oxides) are another important type of minerals in mould that have a permanent

structural charge. Along with surface protons, these minerals have ion-exchangeable sites [512]. Mould surfaces have a wide range of hydroxyl groups with varying reactivities. Among the surfaces that contain terminal –OH groups are alumina surfaces, which are more likely to take an extra proton in acidic solution than surfaces that have only bridging –OH groups. The terminal –OH group resists dissociation to the anionic ≡Al–H^- form despite being a weaker acid, forming a positively charged ≡Al–OH^{+2} site. The terminal –OH group links to metals more strongly than the bridging –OH group after deprotonated [510]. Metal ions can behave as a Lewis acid in aqueous solutions (i.e., an electron acceptor). Lewis salt-type compounds are formed when a surface functional group that donates electron pairs (such as –OH and –COOH) is combined with a metal ion that accepts electron pairs (such as M^{2+}). The functional surface hydroxo groups ≡Fe–OH on an oxide (e.g. ferric oxide) can behave as Lewis bases in deprotonated form (≡Fe–O^-) to bind a Lewis acid metal ion M^{2+} for oxides (e.g. ferric oxide).

$$\equiv Fe - OH + M^{2+} \leftrightarrow \equiv Fe - OM^{2+} + H^{+} \tag{7.2}$$

Complexation with metal oxi anions (such as $HMO^{2-}{}_4$) may result in the release of OH^- ions from the surface :

$$\equiv S - OH + HMO_4^{2-} \leftrightarrow \equiv S - OMO_3H^- + OH^- \tag{7.3}$$

where, ≡S–OH denotes a surface functional group.

While electrostatic bonding is predominant in outer-sphere complexes, coordinate covalent bonding is predominant in inner-sphere complexes, making the latter more stable [513].

$$\equiv S - OH + M\,(OH_2)_n^{2+} \leftrightarrow \equiv S - O\,(H_2O)\,M^{+} + (n-1)\,H_2O + H^{+} \tag{7.4}$$

FTIR analysis of mould was used to determine the active functional groups involved in chemical reactions (Figure 7.4). Before and after the ternary metal ions adsorption, there

were displacements in the mould. Firstly, the intensity of almost all of the infrared bands appeared to decline, and the decreasing vibration intensity indicated that such material had undergone chemical changes [304]. There were evident displacements at 3625.71 to 3636.38 cm^{-1} and 1036.19 to 1038.89 cm^{-1} showed adsorption involves OH and Si-O stretching.

Thus, in the present study ion exchange, electrostatic adsorpion and complexation were the mechanism involved in adsorption of ternary metal ions on mould.

7.5 Comparative Study

Table 7.8 shows a comparison of the percentage removal of mould with other adsorbents.

Table 7.8: Comparison of mould with other adsorbents

Heavy metal	**Adsorbent**	**Wastewater type**	**Initial concentration (mg/L)**	**% Removal**	**Ref**
Nickel (II)	Tea waste	Synthetic	100	62.4	[436]
Copper (II)	*Mangifera indica sawdust*	Synthetic	17.05	81	[514]
Copper (II)	Moringa oleifera activated carbon	Synthetic	5	99.7	[515]
Nickel (II)	African palm fruit Activated carbon	Metal scrap effluent	3.24	89.79	[516]
Copper (II)	African palm fruit Activated carbon	Metal scrap effluent	1.52	92.72	[516]

Nickel (II)	Compost	Synthetic	95	81	[517]
Copper (II)	Compost	Synthetic	102.5	92	[517]
Zinc (II)	Compost	Synthetic	105	66	[517]
Copper (II)	Neem leaf	Synthetic	5	76.8	[338]
Nickel (II)	Neem leaf	Synthetic	5	67.5	[338]
Zinc (II)	Neem leaf	Synthetic	2.5	58.4	[338]
Copper (II)	*Xanthium Pensylvanicum*	Synthetic	10	74	[518]
Nickel (II)	*Xanthium Pensylvanicum*	Synthetic	10	82	[518]
Zinc (II)	*Xanthium Pensylvanicum*	Synthetic	10	20	[518]
Copper (II)	Clay	Synthetic	1000	94	[519]
Nickel (II)	Clay	Synthetic	890	89.55	[519]
Zinc (II)	Clay	Synthetic	975	70.25	[519]
Nickel (II)	**Mould**	**Synthetic**	**50**	**99.26**	**This study**
Copper (II)	**Mould**	**Synthetic**	**50**	**98.91**	**This study**
Zinc (II)	**Mould**	**Synthetic**	**50**	**98.65**	**This study**

It is evident from Table 7.8 that mould is an excellent adsorbent for removing heavy metal ions such as Ni^{2+}, Cu^{2+}, and Zn^{2+} from contaminated water as compared to other adsor-

bents. Though these percentage removals have been obtained in different experimental condition, yet they provide significant and trustworthy information about the efficiencies of various adsorbents.

7.6 Conclusion

The mould was primarily constituted of montmorillonite and non-clay minerals such as quartz and feldspars. The adsorption of Ni^{2+}, Cu^{2+} and Zn^{2+} ions onto mould is found to be dependent on the pH, initial concentration, temperature and contact time. Adsorption revealed that the initial uptake was rapid and equilibrium was achieved within 30 min. The optimum parameters for this study were pH 6, initial metal ion concentration 50 mg/L, contact time 30 minutes and temperature 308 K. The Langmuir maximum adsorption capacity was found to be 0.086 mg/g, 0.045 mg/g, and 0.021 mg/g for Ni^{2+}, Cu^{2+} and Zn^{2+} ions respectively. Thermodynamic study revealed non-spontaneous endothermic process for removal of Ni^{2+}, Cu^{2+} and Zn^{2+} ions onto mould. The best fit of the experimental data in Langmuir isotherm and PSO demonstrated the chemisorption of metal ions with monolayer coverage. The adsorption was based on pore diffusion as evidenced from values of film and pore diffusivity coefficients. The dimensionless numbers (φ, λ and N_k) revealed that the adsorption dynamics of Ni^{2+}, Cu^{2+} and Zn^{2+} ions was transfer controlled process. A thin coating of the mould material inside the water tank will reduce metal concentration in water considerably.